LETTER

Flexible and Transparent SWCNT Electrodes for Alternating Current Electroluminescence Devices

Christian Schrage and Stefan Kaskel*

Department of Inorganic Chemistry, Dresden University of Technology, Mommsenstrasse 6, D-01062 Dresden, Germany, and Department CVD Thin Film Technology, Fraunhofer Institute of Material and Beam Technology, Winterbergstrasse 28, D-01277 Dresden, Germany

ABSTRACT The application of transparent single-walled carbon nanotube (SWCNT) electrodes in rigid and flexible alternating current electroluminescence (ACEL) devices is demonstrated. SWCNT thin-film electrodes (50−160 nm) were made using a spray-coating process suitable for adjusting the transparency and sheet resistance. The dispersing procedure was optimized by comparing the transparency to sheet resistance ratio (*T*/*R*) of the electrodes. The emission intensity was as high as that for indium−tin oxide (ITO)-based ACEL devices with transparencies comparable to those of ITO-coated polymer slides.

KEYWORDS: carbon nanotube • transparent electrode • electroluminescence • thin film

INTRODUCTION

Because of their high resolution and brightness, uniform light emission, and low power consumption together with the possibility of a thin architecture (60−100 μm), alternating current electroluminescence (ACEL) devices have a high potential for commercial application (1). An efficient electroluminescence (EL) phosphor (usually doped zinc sulfide) sandwiched between two electrodes is excited in a strong electric field. Dopant materials (Cu, Al, Cl, Mn, etc.) and phosphors allow color tuning over the whole visible range, and even the creation of white-light-emitting devices has been reported (2). ACEL devices can be used in liquid-crystal-display backlighting such as cellular phones and personal digital assistants and also in large-scale architectural and decorative lighting (2, 3). Up to now, transparent conducting oxides such as indium−tin oxide (ITO) electrodes prepared by cost-intensive sputtering techniques constitute the electrode through which the light is extracted. However, low-temperature deposition techniques compatible with flexible polymer substrates lead to higher sheet resistances and surface roughness of the ITO electrode (4). Moreover, repeated bending of ITO electrodes causes cracking and delamination limiting their flexibility (5). Referring to these facts and the extremely increasing demand on indium, leading to a strong price advance, transparent single-walled carbon nanotube (SWCNT) electrodes seem to be a valuable alternative for ITO-based electrodes for applications with moderate requirements on conductivity.

The recent attention on SWCNTs driven by their exceptional electrical and mechanical properties has led to a large number of applications in the area of optoelectronics and macroelectronics (6−12). A full exploitation of the materials' potential has been accomplished through an effective debundling and dispersion of SWCNT aggregates usually obtained from the production process. Surfactant-assisted ultrasonication is a method to obtain aqueous dispersions with sufficiently high concentrations for solution casting of SWCNT films. The duration and intensity of ultrasonic radiation have to be adjusted carefully because the generation of defects on tube walls or tube shortening may bother the properties negatively. So far, a variety of coating processes such as spin coating (13), drying from a solvent (14), vacuum filtration (15), or spray coating (5) have been proposed in order to produce SWCNT thin films. The resulting two-dimensional random SWCNT networks are highly conductive and mechanically robust, while transparency is retained. The convenience, cost efficiency, and low processing temperatures of the coating methods together with the outstanding properties of SWCNT thin films enabled the generation of several types of devices based on flexible transparent SWCNT electrodes such as organic light-emitting diodes (16, 17), polymer solar cells (18, 19), transparent transistors (20, 21), and even flexible transparent thin-film loudspeakers (22). In our study, we investigate for the first time the use of SWCNTs in ACEL device structures.

EXPERIMENTAL SECTION

SWCNTs (CVD EliCarb high purity; Thomas Swan) were dispersed in a 1 wt % solution of sodium dodecylbenzenesulfonate with the aid of ultrasonic treatment. After centrifugation (2400*g* for 15 min), the homogeneous dispersion was spray-coated on the substrate at 110 and 250 °C for polycarbonate (PC) slides or glass substrates, respectively. After washing with a mixture of ethanol and water, an EL paste containing ZnS:Cu,Cl (Osram) mixed with an organic binder (Laromer PE 56; BASF) was photopolymerized between two SWCNT electrodes (device-type A). For device-type B, the EL phosphor layer

* E-mail: stefan.kaskel@chemie.tu-dresden.de. Phone: 49-351-46333632. Fax: 49-351-46337287.

Received for review April 15, 2009 and accepted July 13, 2009

DOI: 10.1021/am9002588

© 2009 American Chemical Society

Published on Web 07/17/2009

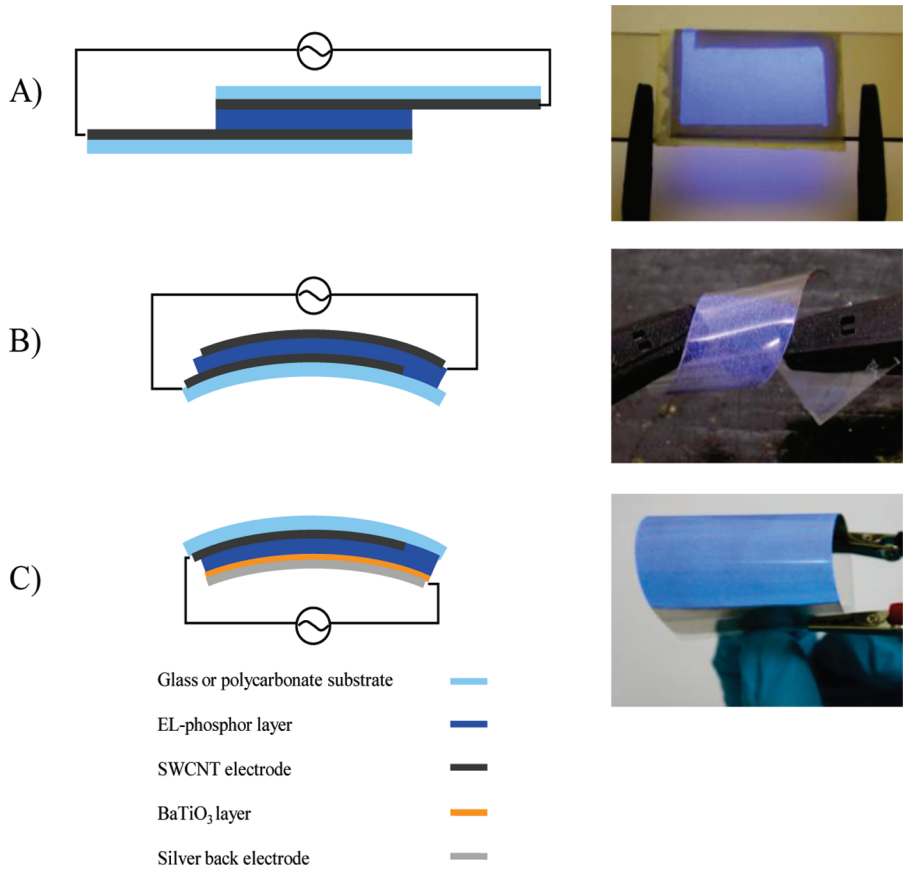

FIGURE 1. Schematic device structures and photographs of rigid (A), flexible (B), and multilayer flexible (C) ACTFEL devices.

was coated on a flexible SWCNT electrode. The SWCNT counter electrode was sprayed directly on the polymerized phosphor layer. An alternative device structure consists of a dielectric $BaTiO_3$ paste (DuPont Luxprint No. 8153) on a silver-coated PC slide followed by the EL-emitting layer. After polymerization, the SWCNT counter electrode was sprayed directly onto the emitting layer.

Transmission spectra and *T*(600) values of dispersions and coated substrates were taken on a Shimadzu UV-1650 PC, while the emission intensity and stability test were evaluated with a Varian Eclipse fluorescence spectrometer. Therefore, the emitting area was limited to 1 cm^2. The sheet resistance of SWCNT coatings was measured via a four-point method on a Keithley 2400 source meter coupled with a four-point probe by Cascade Microtech. The SWCNT film thickness was evaluated with a Dimension 3100 atomic force microscope controlled by a Nanoscope IV SPM controller from Veeco Digital Instruments. Measurements were performed in tapping mode using a Veeco Nanoprobe tip, RTESP7.

RESULTS AND DISCUSSION

The photograph in Figure 1 demonstrates the three different ACEL device structures with SWCNT electrodes under operation. Hence, the CNT network formed on the substrate is flexible and can tolerate mechanical stress caused by bending or stretching without a loss in conductivity. Repeated twisting of the device does not lead to a loss in conductivity or emission efficiency. Even though flexible ITO-based ACEL devices are known and commercially available, their flexibility is limited compared to SWCNT networks because of the brittleness of ITO (23). For proof of principle and for optimization of the dispersing procedure, a rigid (device-type A) and flexible (device-type B) architecture with two SWCNT electrodes was chosen, while the device structure was improved with respect to the lifetime stability and emission intensity through the use of an insulating $BaTiO_3$ barrier layer and a silver backelectrode (device-type C). Additionally, the *transmittance* to *sheet resistance* ratios (*T*/*R* ratios) of SWCNT coatings were compared, revealing information about the quality of the dispersion and tube damage through processing, respectively. The *T*/*R* ratio can be used as a selection criterion for the evaluation of dispersing procedures.

Table 1. Transparency of SWCNT Dispersions (600 nm)[a]

	BS-XXX	TS-XXX-50	TS-XXX-100
XXX = 30	96.4	60.9	18.3
XXX = 60	96.3	33	2.6
XXX = 120	82.6	9.8	0.2
XXX = 180	57.3	2.7	0.2
XXX = 240	37.7	1.4	0

[a] Sample codes: BS-XX bath sonication in XX min; TS-XX-YY tip sonication in XX min with YY relative intensity in percent.

Different dispersing methods (bath and tip sonication) with varying intensities and dispersing durations were used to examine influences on the performance of the SWCNT electrodes. To provide a relative concentration, the dispersion was examined with UV−vis spectroscopy after ultrasonic treatment and centrifugation. The transmission values at 600 nm listed in Table 1 reveal a drastic effect of the

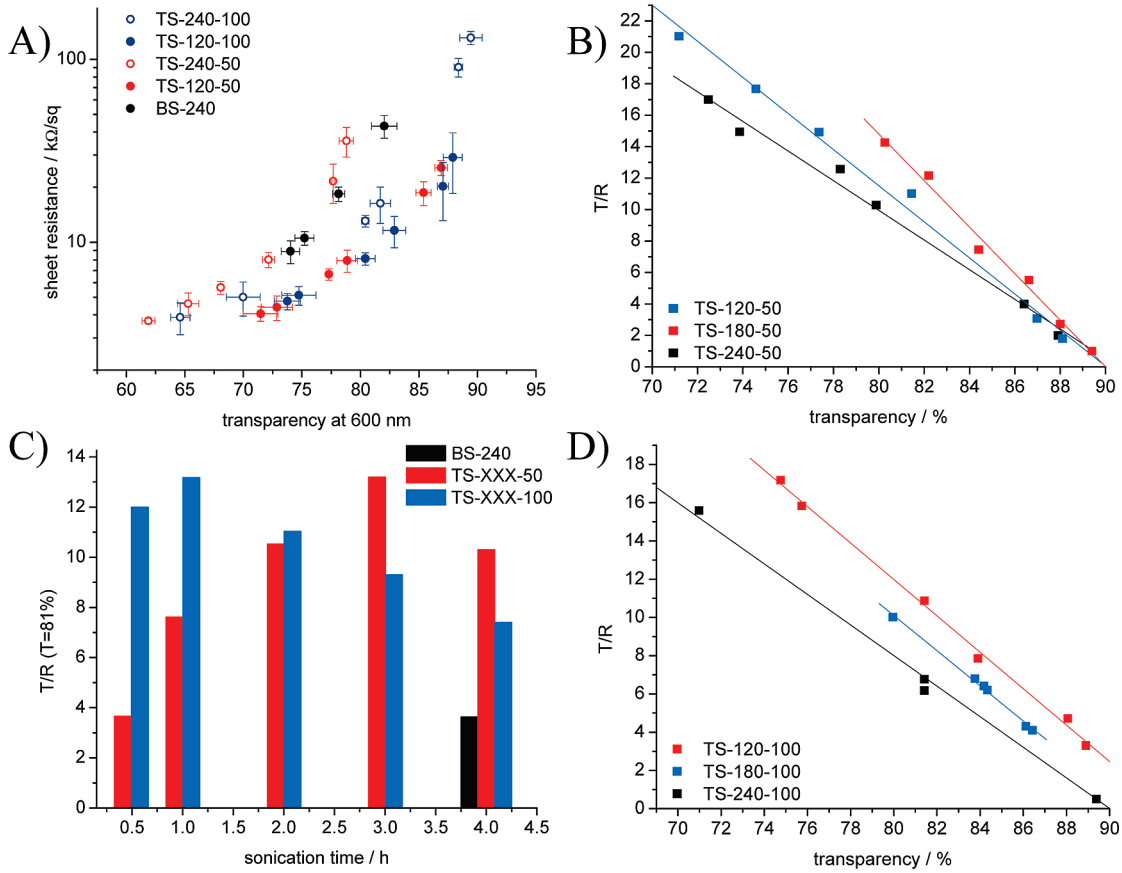

FIGURE 2. (A) *R* vs *T* plots for SWCNT coatings on glass substrates depending on the dispersing procedure (sample codes: BS-XX bath sonication in XX min; TS-XX-YY tip sonication in XX min with YY relative intensity in percent). (B and D) Corresponding *T*/*R* vs *T* plots. (C) *T*/*R* depending on the sonication time and method. All data were obtained from device-type A.

ultrasonic power and time on the SWCNT concentration. While the SWCNT concentration of bath-sonicated samples only slightly increases, resulting in a *T*(600) value of 37% after 4 h of processing, tip sonication leads to high concentrations after a short time, reflected by a quick decrease to 33% (50% intensity) and 3% (100% intensity) transmission for tip-sonicated samples within the first 1 h of processing.

After spray coating, the typical SWCNT film thickness is in the range of 50−160 nm [*T*(600) = 90−65%; see the Supporting Information] as determined at the step edges by atomic force microscopy (AFM). Transparency and sheet resistance are tunable through the quantity of the material sprayed on the surface. A resulting *R* vs *T* plot of selected samples in Figure 2 shows the typical trend of decreasing sheet resistances with decreasing transparencies. (For clarity, only samples sonicated over 120 min are shown. For complete characteristics, see the Supporting Information.) Dispersing SWCNTs in liquids using ultrasound radiation is necessary for debundling but can cause degradation or destruction if the conditions are too harsh. The generated defects on the tube sidewalls as well as tube shortening affect the conductive properties mainly in a negative way, limiting ballistic charge transport inside the SWCNTs. Furthermore, tube shortening leads to an increasing number of contact points between the tubes, causing a higher resistance. On the other hand, an optimal concentration of debundled and nondestructured SWCNT is the key for a good performance of the electrodes. An optimal dispersion leads to effective entangled SWCNT electrodes after the coating process. However, microscopic methods like AFM or scanning electron microscopy (SEM) provide information about the degree of dispersion showing aggregates or dense networks, respectively, but it is difficult to get representative information about tube degradation.

A relative comparison of SWCNT coatings with respect to the processing conditions is possible through the ratio of transmission and sheet resistance *T*/*R*. An increasing *T*/*R* ratio with varying processing parameters like the sonication time or power suggests a lower sheet resistance at the same transmittance, indicating a more efficient percolated CNT network. If larger SWCNT bundles are deposited on the surface, *T*/*R* decreases because the transparency is drastically decreased while the resistance is only slightly affected. In principle, the *T*/*R* ratio should increase with further debundling of SWCNT aggregates and become maximal if the optimal dispersion is reached. Beyond this maximum, a decreasing *T*/*R* ratio suggests the beginning fragmentation of SWCNTs, leading to lower conductivity. The *T*/*R* ratio at a certain transmittance can be determined in a *T*/*R* vs *T* plot, where each CNT coating exhibits a characteristic linear function, shown in Figure 2.

The debundling and dispersion takes place during 3 h of processing with a tip sonicator at 50% relative intensity indicated by increasing *T*/*R*. After the maximum is reached

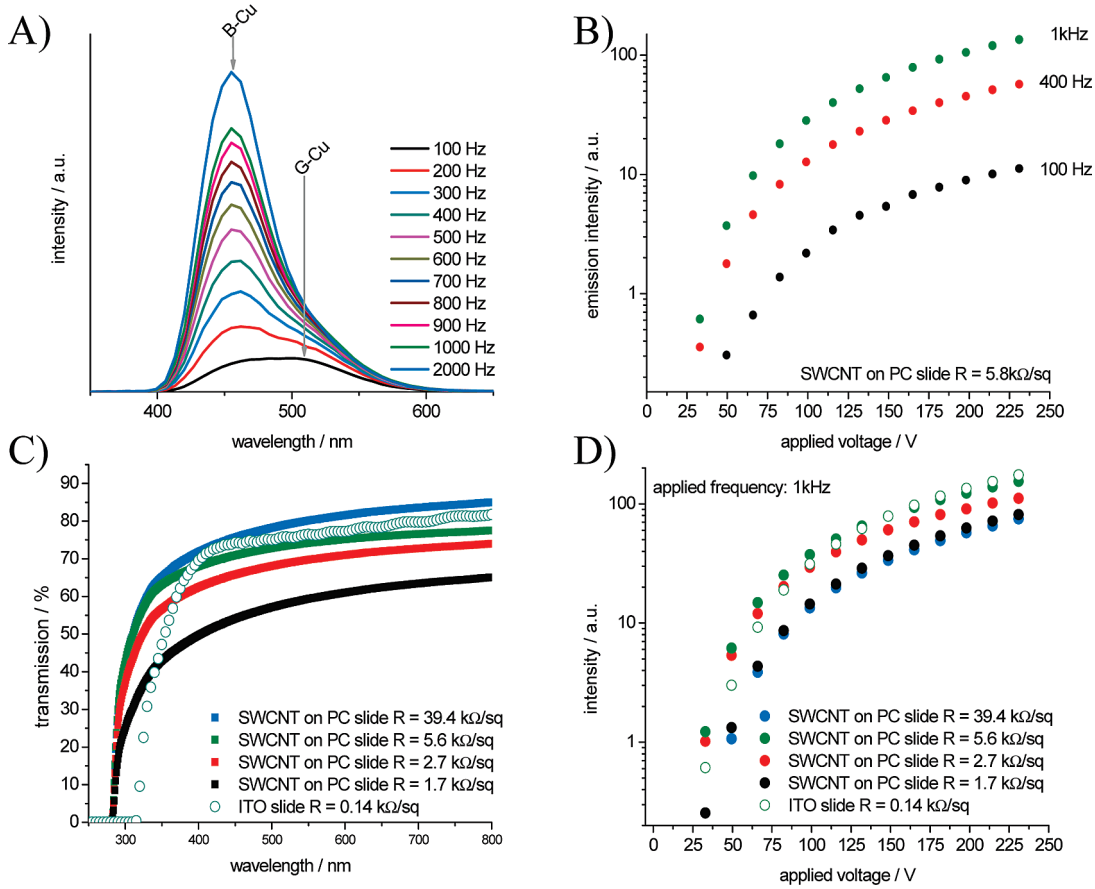

FIGURE 3. (A and B) ACEL characteristics of the used ZnS:Cu,Cl depending on the applied frequency and voltage. (C) Transmission spectra of SWCNT-coated PC slides and an ITO-coated polymer slide. (D) Device characteristics (device-type C) of SWCNT and ITO-based flexible ACTFEL devices. All data were obtained from device-type D.

after 3 h of sonication, *T*/*R* decreases as a result of beginning decomposition. A higher sonication intensity leads to a faster increasing *T*/*R* ratio for TS-XX-100, and it can be observed that the performance of the electrode decreases after passing a maximum at 1 h of processing time. Compared to tip-sonicated samples, bath sonication does not lead to a sufficient debundling of SWCNT aggregates, indicated by the high transparency of the dispersion and the low *T*/*R* value, respectively.

The *T*/*R* method is useful in determining the best dispersing parameters for a certain material. Thus, the maximum transparency and optimal conductivity can be adjusted to exploit the potential of the used CNTs. In our case, a maximal transparency is needed to minimize the absorption of generated EL. Thus, a short (30−60 min) processing time with the tip sonicator at 100% intensity will give the best *T*/*R* ratio at a reasonable dispersing time.

Figure 3 shows EL spectra of SWCNT-based EL devices. A strong dependence of the emission intensity and color on the applied frequency is observed. The emission band consists of two Gaussian components centered at 455 and 511 nm for blue (B-Cu) and green (G-Cu) emission color, respectively.

An increase in the applied frequency leads, on the one hand, to higher emission intensity and, on the other hand, to a shifting ratio between the two emission bands toward the B-Cu band. Thus, the emission color can be easily switched from blue to green by changing the frequency of the applied voltage. The dependence of the emission intensity on the applied voltage is expressed by (24)

$$I = I_0 \exp[-(V_0/V)^{1/2}]$$

The parameters I_0 and V_0 depend on the phosphor particle size, the powder concentration in the organic binder, the dielectric constant of the embedding medium, and finally the thickness of the emitting layer. To explore the influence of the sheet resistance on the emission intensity, the above-mentioned parameters were kept constant and the thickness of the SWCNT layer was varied. Creating a constant electric field over large-area coatings, SWCNTs have to be effectively entangled and have a sufficiently low sheet resistance. Thus, the prior optimized dispersing route (1 h of tip sonication with 100% relative intensity) was chosen for dispersion of the SWCNTs. When the influence of the sheet resistance on the emission performance using device-types A and B was examined, it was found that a sheet resistance of 50 kΩ/□ is sufficient to excite the EL phosphor. This corresponds to a transparency of approximately 90% at 600 nm. Below this onset resistance, the emission intensity increases if the sheet resistance is lowered through a thicker SWCNT layer and decreases again if absorption of the SWCNT electrode becomes too high. This trend was evaluated after improve-

ment of the device structure with respect to the lifetime stability and emission efficiency achieved through the use of a dielectric barrier layer and one silver backelectrode (device C). A dielectric $BaTiO_3$ barrier layer ensures stability, preventing electric breakdowns, on the one hand, and reducing the driving voltage, on the other hand (24). Additionally, $BaTiO_3$ acts as a reflection layer, amplifying the light extraction through the transparent SWCNT front electrode. The spray process can be adopted for coating of the barrier layer and the silver backelectrode as well by dilution of the $BaTiO_3$ paste and silver conducting resin with a proper solvent. Device characteristics depending on the sheet resistance for device-type C are summarized in Figure 3, showing initially an increase in the emission intensity with lower sheet resistance of the SWCNT coating. A maximum emission intensity was observed with a sheet resistance of 5.8 kΩ/□ corresponding to $T(600)$ of 75%. The decrease in the emission intensity below 5.8 kΩ/□ is not proportional to the transparency loss measured with the UV−vis spectrometer. While $T(600)$ decreases from 75% to 60% with increasing SWCNT film thickness, the emission intensity shows a decline of 60%. Because of the larger emitting area, this fact can be attributed to light scattering effects rather than to absorption. Compared with an ITO reference device with an $T(600)$ value of 77% and a sheet resistance of more than 1 order of magnitude lower, a comparable emission intensity and an onset voltage of approximately 35 V (1 kHz of applied frequency) can be achieved. Thus, the EL phosphor is excited to its maximum intensity, while lowering the sheet resistance of the SWCNT electrodes does not lead to higher emission intensity because absorption of the generated light comes to the fore with increasing SWCNT layer thickness. The emission stability was tested for 10 days under ambient conditions by applying 200 V and 1 kHz. Within this period, no loss in the emission intensity was observed.

CONCLUSION

In summary, the use of SWCNT electrodes as an alternative for ITO in rigid and flexible ACEL devices has been demonstrated, leading to a number of advantages. With a comparable device efficiency and quality, cost-intensive sputter techniques or high-temperature treatment can be replaced by low-temperature solution-casting procedures, whereby spray coating is compatible with established large-area coating techniques known from lacquer application. Additionally, the spray process is not limited to flat substrate shapes, and hence a variety of substrates can be chosen. A high conductivity of ITO is not necessary in the case of ACEL to achieve a maximum intensity of the EL phosphor used, while SWCNT electrodes lead to highly flexible, mechanically robust device architectures.

Acknowledgment. We thank Petra Pötschke from the Leibniz-Institute of Polymer Research Dresden for providing Thomas Swan EliCarb SWCNTs.

Supporting Information Available: Transmission at 600 nm and the corresponding sheet resistance of SWCNT coatings on a glass substrate, the thickness dependence of the transmission, and a SEM picture of a representative SWCNT network made of a well-dispersed sample (TS-60−50). This material is available free of charge via the Internet at http://pubs.acs.org.

REFERENCES AND NOTES

(1) Tiwari, S.; Tiwari, S.; Chandra, B. P. *J. Mater. Sci.: Mater. Electron.* **2004**, *15* (9), 569–574.
(2) Park, J. H.; Lee, S. H.; Kim, J. S.; Kwon, A. K.; Park, H. L.; Han, S. D. *J. Lumin.* **2007**, *126* (2), 566–570.
(3) Vlaskin, V. I.; Vlaskina, S. I.; Koval, O. Y.; Rodionov, V. E.; Svechnikov, G. S. *Semicond. Phys., Quantum Electron. Optoelectron.* **2007**, *10* (2), 16–20.
(4) Aguirre, C. M.; Auvray, S.; Pigeon, S.; Izquierdo, R.; Desjardins, P.; Martel, R. *Appl. Phys. Lett.* **2006**, *88* (18), 183104/1–183104/3.
(5) Kaempgen, M.; Duesberg, G. S.; Roth, S. *Appl. Surf. Sci.* **2005**, *252* (2), 425–429.
(6) Avouris, P. *Acc. Chem. Res.* **2002**, *35* (12), 1026–1034.
(7) Charlier, J.-C.; Blase, X.; Roche, S. *Rev. Mod. Phys.* **2007**, *79* (2), 677–732.
(8) Han, J. *Carbon Nanotubes* **2005**, 1–24.
(9) Hatton, R. A.; Miller, A. J.; Silva, S. R. P. *J. Mater. Chem.* **2008**, *18* (11), 1183–1192.
(10) SlaninaZ. *Carbon Nanotubes: Properties and Applications*; O'Connell, M. J., Ed.; Taylor & Francis Group, Boca Raton, FL, 2008; Vol. 16, p 88.
(11) Stach, E. *Nat. Nanotechnol.* **2008**, *3* (10), 586–587.
(12) White, C. T.; Todorov, T. N. *Nature (London)* **1998**, *393* (6682), 240–242.
(13) Meitl, M. A.; Zhou, Y.; Gaur, A.; Jeon, S.; Usrey, M. L.; Strano, M. S.; Rogers, J. A. *Nano Lett.* **2004**, *4* (9), 1643–1647.
(14) Sreekumar, T. V.; Liu, T.; Kumar, S.; Ericson, L. M.; Hauge, R. H.; Smalley, R. E. *Chem. Mater.* **2003**, *15* (1), 175–178.
(15) Wu, Z.; Chen, Z.; Du, X.; Logan, J. M.; Sippel, J.; Nikolou, M.; Kamaras, K.; Reynolds, J. R.; Tanner, D. B.; Hebard, A. F.; Rinzler, A. G. *Science (Washington, D.C.)* **2004**, *305* (5688), 1273–1277.
(16) Ryu, K.; Zhang, D.; Liu, X.; Polikarpov, E.; Thompson, M.; Zhou, C. *Mater. Res. Soc. Symp. Proc.* **2006**, *936E*, 0936L04−04.
(17) Li, J.; Hu, L.; Wang, L.; Zhou, Y.; Gruener, G.; Marks, T. J. *Nano Lett.* **2006**, *6* (11), 2472–2477.
(18) Rowell, M. W.; Topinka, M. A.; McGehee, M. D.; Prall, H.-J.; Dennler, G.; Sariciftci, N. S.; Hu, L.; Gruner, G. *Appl. Phys. Lett.* **2006**, *88* (23), 233506/1–233506/3.
(19) Du Pasquier, A.; Unalan, H. E.; Kanwal, A.; Miller, S.; Chhowalla, M. *Appl. Phys. Lett.* **2005**, *87* (20), 203511/1–203511/3.
(20) Artukovic, E.; Kaempgen, M.; Hecht, D. S.; Roth, S.; Gruener, G. *Nano Lett.* **2005**, *5* (4), 757–760.
(21) Bradley, K.; Gabriel, J.-C. P.; Gruener, G. *Nano Lett.* **2003**, *3* (10), 1353–1355.
(22) Xiao, L.; Chen, Z.; Feng, C.; Liu, L.; Bai, Z.-Q.; Wang, Y.; Qian, L.; Zhang, Y.; Li, Q.; Jiang, K.; Fan, S. *Nano Lett.* **2008**, *8* (12), 4539–4545.
(23) Leterrier, Y.; Medico, L.; Demarco, F.; Manson, J. A. E.; Betz, U.; Escola, M. F.; Kharrazi Olsson, M.; Atamny, F. *Thin Solid Films* **2004**, *460* (1−2), 156–166.
(24) Shigeo, S.; Yen, W. M. *Phosphor Handbook*; CRC Press LLC: Boca Raton, FL, 1999.

AM9002588